UC Santa Cruz

UC Santa Cruz Previously Published Works

Title

Dissolved hydrogen and nitrogen fixation in the oligotrophic North Pacific Subtropical Gyre

Permalink

https://escholarship.org/uc/item/0430307m

Journal

Environmental Microbiology Reports, 6(1)

ISSN

1758-2229

Authors

Wilson, Samuel T
Valle, Daniela A
Robidart, Julie C
et al.

Publication Date

2014-02-01

DOI

10.1111/1758-2229.12127

Peer reviewed

eScholarship.org Powered by the California Digital Library
University of California

Dissolved hydrogen and nitrogen fixation in the oligotrophic North Pacific Subtropical Gyre

Samuel T. Wilson*[1,2], Daniela A. del Valle[1,2], Julie C. Robidart[2,3], Jonathan P. Zehr[2,3] and David M. Karl[1,2]

[1] Department of Oceanography, School of Ocean and Earth Science and Technology, University of Hawaii, Honolulu, Hawaii 96822

[2] Center for Microbial Oceanography: Research and Education, University of Hawaii, 1950 East-West Road, Honolulu, Hawaii 96822

[3]Ocean Sciences, University of California, Santa Cruz, California 95064

*corresponding author

Tel: 808-956-0565; Fax: 808-956-0581. Email: stwilson@hawaii.edu

Summary

The production of hydrogen (H_2) is an inherent component of the biological dinitrogen (N_2) fixation process with the theoretical stoichiometry predicting an equimolar production of H_2 for every mole of N_2 fixed. However, while the stoichiometry of N_2 fixation can be evaluated in high biomass cultures of diazotrophs, conducting the relevant measurements for a field population is more complex. Independent measurements of N_2 fixation, H_2 consumption, and dissolved H_2 concentrations were performed on surface water samples collected in the oligotrophic North Pacific Ocean to constrain the cycling of H_2 associated with N_2 fixation. The quantity of H_2 consumed by microbial oxidation was equal to 1-7% of ethylene produced during the acetylene reduction assay and to 11-63% of $^{15}N_2$ assimilation. Varying abundance of *Crocosphaera* and *Trichodesmium* as revealed by *nifH* gene abundance broadly corresponded with diel changes observed in both N_2 fixation and H_2 oxidation. However no corresponding changes were observed in the dissolved H_2 concentrations which remained consistently supersaturated (147–560%) relative to atmospheric equilibrium. The results from this field study allow the efficiency of H_2 cycling by natural populations of diazotrophs to be compared to their cultured representatives. The findings indicate that the extent to which dissolved H_2 concentrations correspond to N_2 fixation in the open ocean may depend less upon the species of diazotrophs present in the water column and more upon relevant environmental parameters *e.g.* light intensity or the presence of other H_2-metabolizing microorganisms.

Introduction

In the surface waters of the tropical and subtropical open ocean, dissolved H_2 concentrations typically range from 1–3 nmol l^{-1}, equivalent to 300–900% supersaturation relative to atmospheric equilibrium (Herr *et al*., 1984; Conrad and Seiler, 1988; Moore *et al*., 2009). The magnitude of the dissolved H_2 pool is determined by the 'oceanic H_2 cycle' which reflects the balance between production and consumption processes. As such, the main source of H_2 is considered to be biological dinitrogen (N_2) fixation (Scranton *et al*., 1987; Herr *et al*., 1984; Moore *et al*., 2009) whereby N_2 is reduced to ammonia (NH_3), as shown in Equation 1:

(Eq. 1) $N_2 + 8\ H^+ + 8\ e^- + 16\ ATP \rightarrow 2\ NH_3 + H_2 + 16\ ADP + 16\ Pi$

where ADP and ATP are adenosine-5'-diphosphate and adenosine-5'-triphosphate respectively, H^+ is hydrogen ion, e^- is electron, and Pi is inorganic phosphorus (Simpson and Burris 1984).

While N_2 fixation is more commonly measured than H_2 production, it is unwise to use the theoretical stoichiometry predicted in Eq. 1 to provide an estimate of H_2 production associated with nitrogenase activity. This is due to several inherent issues associated with H_2 cycling linked to N_2 fixation, as listed below:

(i) Measurements of H_2 production alongside measurements of N_2 fixation are always less than the equimolar stoichiometry predicted in Equation 1 (Schubert and Evans, 1976; Wilson *et al*., 2010). This is because all diazotrophs contain uptake hydrogenases that re-assimilate a variable portion of H_2 released during N_2 fixation to conserve energy (Burns and Hardy, 1975, Tamgnini *et al*., 2007).

(ii) Rates of net H_2 production by diazotrophs appear to be highly species-specific. Laboratory-maintained cultures of two diazotrophs, *Crocosphaera* and *Trichodesmium* produce H_2 at approximately 1 and 25% of their respective rates of N_2 fixation, as measured by the acetylene reduction (AR) assay (Wilson *et al*. 2010). The comparatively high rates of net H_2 production by *Trichodesmium* are a consequence of the cells fixing N_2 during the day-time as the supply of photosynthetically-derived energy and reductant decreases the need to re-assimilate the H_2 as an energy source, resulting in an increase of net H_2 production (Wilson *et al*., 2012b). By comparison, *Crocosphaera* fixes N_2 during the dark period restricting the supply of cellular energy to nitrogenase from the respiration of photosynthetically-fixed carbon (Waterbury *et al*., 1988; Berman-Frank *et al*., 2007). This causes a greater demand for the energy and reductant produced from oxidizing H_2 and therefore decreases the net H_2 production (Wilson *et al*., 2010).

(iii) Field measurements of N_2 fixation can be conducted using the $^{15}N_2$ assimilation technique or the AR assay. The $^{15}N_2$ tracer technique is considered to be a measure of net N_2 fixation (Montoya *et al*., 1996; Mulholland *et al*., 2004). The AR assay measures total nitrogenase activity by quantifying the reduction of acetylene (C_2H_2) to ethylene (C_2H_4) and therefore represents an indirect assay of N_2 fixation (Burris, 1975). Because H_2 production would be expected to scale on gross N_2 fixation (Eq. 1), the AR assay could represent a better correlative measurement to comparing N_2 fixation and H_2 cycling.

Due to the issues listed above, to define the role of N_2 fixation in the global H_2 cycle (*e.g*. Price *et al*., 2007) it is imperative to conduct field measurements of both N_2 fixation and H_2 production. In this study, simultaneous measurements of N_2 fixation, biological H_2 consumption, and dissolved H_2 concentrations were conducted in the surface waters of

the open ocean where diazotrophs are present. Results are presented of the diazotrophic community composition (as measured by *nifH* gene abundance and diversity), rates of net and gross N_2 fixation (as measured by $^{15}N_2$ tracer assimilation and AR assay, respectively), H_2 concentrations, and H_2 oxidation rates (using $^{3}H_2$ as a tracer). Quantitative interpretation of the field data is aided by the recent measurement of net H_2 production and N_2 fixation in laboratory cultures of diazotrophs to infer the relative contribution of the representative marine N_2 fixing microorganisms to the oceanic H_2 cycle.

Results and discussion

Sampling overview

The oceanographic cruise was located approximately 250 km north of Oahu, Hawaii in the North Pacific Subtropical Gyre (NPSG) and occurred between 6 and 21 September 2011. The sampling stations were occupied along north-western edge of an anticyclonic eddy spanning a total distance of 90 km and the subsequent westward section of the cruise track which spanned 80 km. Vertical profiles of dissolved H_2 were conducted daily alongside biogeochemical and hydrographic measurements. Biological rate measurements of N_2 fixation and H_2 consumption were conducted at 3 sampling stations: Station (Stn) 3, 7, and 13 which were sampled on the 7, 9, and 18 September 2011, respectively. Descriptions of the hydrographic conditions and biogeochemical properties of the water column are available in the accompanying Supplementary Information and also online at http://hahana.soest.hawaii.edu/cmorebiolincs/biolincs.html.

Dissolved H_2 concentrations

Dissolved H_2 concentrations were super-saturated with respect to atmospheric equilibrium in the upper 75 m of the water column (Fig. 1). Overall, dissolved H_2 concentrations in the surface mixed layer (0–45 m) ranged from 0.5–1.9 nmol l^{-1}, with an average concentration of 0.83 nmol l^{-1}, equivalent to 250% supersaturation. On four separate occasions the concentrations of dissolved H_2 in the mixed layer exceeded 1 nmol l^{-1} (Fig. 1). The concentrations of H_2 measured in surface seawater during this cruise are consistent with measurements in other marine environments (e.g. the Atlantic, Mediterranean, and Pacific Ocean) revealing a persistent supersaturation of dissolved H_2 in the near-surface seawater (Conrad and Seiler 1988, Herr *et al*., 1984, Moore *et al*., 2009, Scranton *et al*., 1982). At depths exceeding 75 m a progressive depletion in H_2 concentrations was observed with values approaching undersaturation with respect to atmospheric equilibrium by a depth of 100 m. Vertical profiles of N_2 fixation in the NPSG measured on previous occasions (Church *et al*., 2009, Grabowski *et al*., 2008) similarly show a decrease at 75 m, providing indirect evidence that the dissolved H_2 is derived from nitrogenase activity.

N_2 fixation

N_2 fixation rate measurements, determined by both the $^{15}N_2$ tracer assimilation and the AR assay, were conducted at Stn 3, 7 and 13. The overall temporal pattern of N_2 fixation changed between the stations from an initial prevalence during the night-time, to a subsequent dominance during the day-time. Specifically, rates of $^{15}N_2$ assimilation during the night-time (0.22 nmol l^{-1} h^{-1}) exceeded the day-time (0.08 nmol l^{-1} h^{-1}) at Stn 3

(Fig. 2A). In contrast, at Stn 13, rates of $^{15}N_2$ assimilation in whole seawater were highest (0.26 nmol l^{-1} h^{-1}) during the day-time, compared to the rates during the night-time (0.04 nmol l^{-1} h^{-1}) (Fig. 2C). No significant difference was observed between the day-time and night-time measurements of N_2 fixation at Stn 7. At all sampling stations, the rate of $^{15}N_2$ assimilation in whole seawater samples exceeded the comparative rates in the accompanying <10 µm size fractionated seawater samples. Comparison of the <10 µm size fraction across the three stations reveals low variability in the rate of $^{15}N_2$ assimilation (0.04–0.06 nmol l^{-1} h^{-1}) during the day-time. In contrast, night-time rates of $^{15}N_2$ assimilation for the <10 µm size fraction varied by an order of magnitude, decreasing from 0.14 nmol l^{-1} h^{-1} at Stn 3, to 0.01 nmol l^{-1} h^{-1} at Stn 13 (Fig. 2A-C).

AR was measured on whole seawater samples and a significant increase in C_2H_4 concentrations was always detected during the 3–4 h incubations (Fig. 2D-F). The rates of C_2H_4 production support the $^{15}N_2$ assimilation measurements with higher rates during the night-time (2.9 nmol l^{-1} h^{-1}) compared to the day-time (1.8 nmol l^{-1} h^{-1}) at Stn 3. Furthermore, at Stn 13, the diel pattern of C_2H_4 production changed with day-time (3.3 nmol l^{-1} h^{-1}) exceeding night-time (0.4 nmol l^{-1} h^{-1}) (Fig. 2F). Overall, the ratio of C_2H_4 to $^{15}N_2$ assimilation varied from 9–22 which exceeds the theoretical ratio of 3:1 (Capone 1993) by 3–7 fold. It should be noted that the theoretical ratio of 3:1 is based on the difference between 2 hydrogen ions required to reduce C_2H_2 to C_2H_4 and 6 hydrogen ions needed to reduce N_2 to $2NH_3$. The reasons for the discrepancies between the theoretical and observed ratios have previously been discussed (*e.g.* Graham *et al.*, 1980) and focus mainly on the excretion of N from the cell and the role of H_2. There is insufficient data in this study to contribute to this discussion, however we do note from our work and the

relevant literature that there is increased discrepancy in the C_2H_4: $^{15}N_2$ assimilation ratio in field measurements compared to culture-based analyses. Furthermore there is a lack of experimental testing on the effect of key environmental parameters on the C_2H_4: $^{15}N_2$ assimilation ratio *e.g*. light intensity or nutrient concentrations (Mague *et al*., 1977).

Diazotroph community structure

Representative N_2 fixing microorganisms in the open ocean include: (i) the filamentous, non-heterocystous cyanobacterium *Trichodesmium*, (ii) the heterocystous cyanobacteria (e.g. *Richelia* and *Calothrix*) that form symbioses with eukaryotic algae, and (iii) unicellular cyanobacteria including Group A (termed UCYN-A) and Group B (e.g. *Crocosphaera*) (Mague *et al*., 1977; Carpenter and Romans 1991; Zehr *et al*., 2001). The analysis of *nifH* gene abundances revealed Group B was the most abundant diazotroph for the first two sampling occasions (Stn 3 and 7), with 4.3×10^5 and 1.3×10^6 gene copies l^{-1}. At the third sampling site (Stn 13), *nifH* gene copies of Group B decreased to 2.9×10^4 gene copies l^{-1}, in contrast to *Trichodesmium nifH* gene copies which increased to a maximum of 1.6×10^6 gene copies l^{-1} (Fig. 2). The shift from a Group B-dominated to a *Trichodesmium*-dominated diazotroph community between Stn 3 and 13, respectively, could help account for the change in the pattern of N_2 fixation. The unicellular *Crocosphaera* fixes N_2 in the dark and rates of N_2 fixation were highest during the night-time when *Crocosphaera* gene copies were most abundant. Two other groups of diazotrophs were present at lower abundances throughout the cruise; UCYN-A *nifH* abundance ranged from 1.6×10^3 to 1.9×10^5 gene copies l^{-1} and the total

heterocystous cyanobacterial gene copies were the lowest of all *nifH* gene groups measured with a maximum abundance of 6.2×10^3 gene copies l^{-1} at Stn 13.

Microbial consumption of H_2

Biological $^3H_2$ oxidation was measured during the day and night-time, alongside N_2 fixation rate measurements at Stn 3 and 13. Overall, the rates of biological $^3H_2$ oxidation ranged from 15 to 42 pmol H_2 l^{-1} h^{-1} (Table 1). At Stn 3, night-time rates of biological $^3H_2$ oxidation (25 pmol H_2 l^{-1} h^{-1}) exceeded day-time rates (15 pmol H_2 l^{-1} h^{-1}) by 66%. In contrast, at Stn 13 the day-time rates of biological $^3H_2$ oxidation (42 pmol H_2 l^{-1} h^{-1}) were 68% higher than night-time (25 pmol H_2 l^{-1} h^{-1}) (Table 1). In this respect, the temporal variability in biological $^3H_2$ oxidation rates reflect the temporal patterns observed in the rate of $^{15}N_2$ assimilation and the AR assay. The measured rates of $^3H_2$ oxidation were equivalent to 11-63% of $^{15}N_2$ assimilation and 1-7% of C_2H_4 production as measured by the AR assay.

Previous measurements of biological H_2 consumption have been reported from other aquatic habitats including coastal seawater (Punshon *et al*., 2007), shallow lakes (Conrad *et al*., 1983), and river systems (Paerl 1982). These previous studies have revealed H_2 turnover times ranging from <1 h in a eutrophic shallow lake (Conrad *et al*., 1983) to 2–3 days in high-latitude coastal seawater (Punshon *et al*., 2007). In comparison, the H_2 turnover times measured in this study at two sampling stations ranged from 22–40 h (Table 1).

Estimation of the production and consumption of H_2 associated with N_2 fixation

197 The measured rates of N_2 fixation using the AR assay at Stn 3 and 13 were used to
198 estimate the production of H_2 derived from nitrogenase (Table 2). We use laboratory-
199 derived measurements of net H_2 production by *Trichodesmium* and *Crocosphaera*
200 cultures described in the Introduction to provide upper and lower boundaries for H_2
201 production. Therefore in contrast to Price *et al*. (2007) who estimated net H_2 production
202 at 55% of N_2 fixation in the marine environment, we set maximum and minimum net H_2
203 production rates at 25% and 1% of C_2H_4 production, respectively. The resulting
204 estimates of net H_2 production range from 0.004 to 0.84 nmol H_2 l^{-1} h^{-1} in the upper water
205 column. Furthermore, the calculations indicate that N_2 fixation can replenish the
206 dissolved H_2 pool in as little as 1 h and extending up to 34 hrs, with the exception of 19
207 September during the night time which has an excessively long upper estimate of 245 h
208 (Table 2).
209 The estimates of net H_2 production in surface seawater as listed in Table 2 can be
210 compared with the biological $^3H_2$ oxidation measurements which were conducted on the
211 same seawater samples (Table 1). The rates of $^3H_2$ oxidation were equivalent to 0.8 – 6.6
212 % of the AR assay (Table 2) indicating biological consumption was equivalent to the
213 lower end of estimated rates of net H_2 production *i.e*. comparable to rates of net H_2
214 production by *Crocosphaera*. This suggests that concentrations of dissolved H_2 may
215 increase in the presence of *Trichodesmium* and stimulate the diel cycles of H_2 in surface
216 seawater as observed by Herr *et al*. (1984) in the South Atlantic. However in this study,
217 the increase in *Trichodesmium* abundance was not matched by an increase in net H_2
218 concentrations (Fig. 1) suggesting that field populations of *Trichodesmium* may re-
219 assimilate more of the H_2 produced via nitrogenase compared to their cultured counter-

parts and are therefore more energetically efficient. Alternatively, other sinks of H_2 in the upper ocean may contribute to the loss of dissolved H_2 and these are considered in the next section.

H_2 cycling in the open ocean

The oceanic H_2 cycle depends not only on biological production and consumption as discussed with reference to diazotrophs, but also physical forcing mechanisms. The physical processes can be considered with respect to the sink terms for H_2, comparing estimates of air-sea gas exchange and downwards diffusion with biological oxidation. The downward diffusion of H_2 can be estimated from the concentration gradient between depths of 45 and 75 m, using the vertical eddy diffusion coefficient reported by Ledwell *et al*. (1993) (Table 3). The flux of H_2 to the atmosphere can be estimated according to Equation 2, where *S* is the Bunsen solubility coefficient (Wiesenburg and Guinasso, 1979), Δp is the difference in partial pressure (p) between the atmosphere and ocean, and k is the transfer velocity. An atmospheric H_2 concentration of 0.53 ppmv was used in the flux calculations (Novelli *et al*., 1999). The transfer velocity (k) was calculated according to Wanninkhof (1992) (Equation 3) where U is the wind speed (m sec^{-1}) normalized to 10 m above the sea surface and *Sc* represents the Schmidt number for H_2 at *in situ* seawater temperature and salinity (Jähne *et al*., 1987).

(2) $F = k \cdot S \cdot \Delta p$

(3) $k = 0.31\ U^2\ (Sc/660)^{-0.5}$

To obtain depth-integrated estimates of H_2 consumption we used historical measurements of N_2 fixation profiles at Stn ALOHA (HOT cruises #202-213) to calculate

the relationship between N_2 fixation measurements at 25 m and 0-45 m depth integrated values ($y=46.12x + 23.8$, $r^2=0.82$). The conversion factor was applied to the rates of N_2 fixation (Fig.1) using the percentage of AR assay and $^{15}N_2$ assimilation (Table 1) to provide a lower and upper estimate of biological H_2 consumption respectively, integrated across the 0-45 m depth horizon. While there is approximately an order of magnitude difference between the upper and lower estimates of biological consumption (Table 3), the median values for turnover times compare favorably with the rates of H_2 consumption calculated from the $^3H_2$ oxidation measurements for discrete seawater samples collected from 25 m (Table 1). It is evident that for this time period, biological consumption and downward diffusion represented the main loss pathways for dissolved H2 in the upper ocean. The estimated flux of H_2 to the atmosphere ranged from 0.03 - 0.33 μmol m^{-2} h^{-1} (Table 3) and should be considered a low estimate of H_2 loss to the overlying atmosphere due to the predominantly low wind speeds (<5 m sec^{-1}) during the cruise.

Conclusion

During a 10 day sampling period in the NPSG, dissolved H_2 concentrations were 147–560% supersaturated with respect to atmospheric equilibrium. Measured rates of $^{15}N_2$ assimilation and AR revealed a change in the prevalence of N_2 fixation from night-time to day-time, which was accompanied by a decrease in the abundance in Group B *nifH* gene copies, and an increase in the abundance of *Trichodesmium nifH* gene copies. Prior to this study it was hypothesized that varying abundance of larger, day-time N_2 fixing microorganisms *e.g. Trichodesmium* might influence the dissolved pool of H_2 in surface seawater due to their relatively high rates of net H_2 production (Wilson *et al.*,

2010). However the absence of varying dissolved H_2 concentrations indicate that field populations of *Trichodesmium* may be more efficient at recycling H_2 compared to laboratory cultures. Biological H_2 oxidation measurements in seawater sampled from 25 m depth indicate that H_2 production needed to exceed 1-6% of C_2H_4 production to cause an increase in the ambient pool of dissolved H_2 (Table 1). This is considerably lower than in laboratory-maintained *Trichodesmium* cultures where the rate of net H_2 production was equivalent to 25% of C_2H_4 production (Wilson *et al*., 2012b). Using either the AR assay or the $^{15}N_2$ assimilation technique caused approximately 1 order of magnitude variability when calculating the efficiency of H_2 cycling. We consider the AR assay to be more representative of nitrogenase activity but recognize that it is an indirect measurement and not widely used in oceanographic studies on non-concentrated seawater samples. Comparison of the loss mechanisms for dissolved H_2 in the upper ocean indicated that biological oxidation represented the most prevalent sink compared to downward diffusion and flux to the atmosphere (Table 3).

It should be noted that oceanic H_2 cycling is not limited to diazotrophs, and opportunistic H_2-oxidizing microorganisms *e.g*. aerobic anoxygenic photosynthetic bacteria and heterotrophic bacteria will also metabolize H_2. Furthermore, other sources of H_2 such as photochemical degradation of dissolved organic matter (Punshon and Moore 2008) and fermentation (Schropp *et al*., 1987) should be considered when considering H_2 cycling in the upper water column. Nonetheless, this study confirms that wherever diazotrophs occur in the natural environment, the ecosystem becomes enriched in dissolved H_2 (Conrad 1988) although the cycling of H_2 is more subtle than suggested from laboratory cultures of diazotrophs.

289

290 **Method**

291 Dissolved H_2 concentrations were measured with a reduced gas analyzer (Peak
292 Laboratories, Mountain View) adapting the method of Moore *et al*. (2009). The rate of
293 H_2 consumption was quantified by measuring the production of ^3H_2O from tracer
294 additions of $^3H_2$ as previously used in laboratory cultures of diazotrophs (Chan *et al*.,
295 1980) and environmental microbial assemblages (Paerl, 1983). To determine the rate of
296 N_2 fixation, measurements of $^{15}N_2$ assimilation and AR were carried out as described in
297 Wilson et al. (2012a). The *nifH* gene abundance was quantified using the methodological
298 protocols previously published by Moisander *et al*. (2010). Full descriptions of all the
299 analytical methods for measuring H_2 and N_2 fixation and also the accompanying
300 hydrographic datasets are in the Supplementary Information.

301

302 **Acknowledgements**

303 We are grateful to the numerous scientists who contributed to the success of the C-
304 MORE BioLINCS cruise, and in particular thank Blake Watkins, Tara Clemente, Ben
305 Rubin, Ariel Rabines, Daniela Böttjer, Susan Curless who assisted with sample collection
306 and analysis. François Ascani helped with modeled FSLE projections to aid cruise
307 planning. We also thank the R/V Kilo Moana captain and crew for their support. This
308 research was supported by the National Science Foundation supported Center for
309 Microbial Oceanography: Research and Education (C-MORE) (EF0424599 to D.M.K.,
310 P.I.), NSF Grant OCE-1153656 (D.M.K., P.I.) and the Gordon and Betty Moore
311 Foundation Marine Microbiology Investigator awards to J.P.Z. and D.M.K., including the

312 MEGAMER facility grant by the Gordon and Betty Moore Foundation..

References

Berman-Frank, I., Quigg, A., Finkel, Z.V., Irwin, A.J., and Haramaty, L. (2007) Nitrogen-fixation strategies and Fe requirements in cyanobacteria. *Limnol Oceanogr* **52**: 2260–2269.

Burns, R.C., and Hardy, R.W.F. (1975) Nitrogen fixation in bacteria and higher plants. Molecular Biology, Biochemistry, and Biophysics. Vol 21. Springer Verlag, Heidelberg, Berlin. pp.1–189.

Burris RH (1975) The acetylene-reduction technique. In *Nitrogen fixation by free-living microorganisms*. Stewart, W.D.P. (ed) Cambridge University Press, New York, p 249–257.

Capone, D.G. (1993) Determination of nitrogenase activity in aquatic samples using the acetylene reduction procedure. In *Handbook of microbial methods in aquatic microbial ecology.* Kemp, P.F., Sherr, B.F., Sherr, E.B., and Cole, J.J. (ed) Lewis Publishers, Boca Raton, Florida, p 621–631.

Carpenter, E.J., and Romans, K. (1991) Major role of the cyanobacterium *Trichodesmium* in nutrient cycling in the North Atlantic Ocean. *Science* **254**: 1356–1358.

Chan, Y.K., Nelson, L.M., and Knowles, R. (1980) Hydrogen metabolism of *Axospirillum brasilense* in nitrogen-free medium. *Can J Microbiol* **26**: 1126–1131.

Church, M.J., Mahaffey, C., Letelier, R.M., Lukas, R., Zehr, J.P., and Karl, D.M. (2009) Physical forcing of nitrogen fixation and diazotroph community structure in the North Pacific subtropical gyre. *Global Biogechem Cycles* **23:** GB2020, doi:10.1029/2008GB003418.

335 Conrad, R. (1988) Biogeochemistry and ecophysiology of atmospheric CO and H_2.
336 *Advances in Microbial Ecol* **10**: 231–283.
337 Conrad, R., Aragno, M., and Seiler, W. (1983) Production and consumption of hydrogen
338 in a eutrophic lake. *Appl Environ Microbiol* **45**: 502–510.
339 Conrad, R., and Seiler, W. (1988) Methane and hydrogen in seawater (Atlantic Ocean).
340 *Deep-Sea Res* **35**: 1903–1917.
341 Grabowski, M.N.W., Church, M.J., and Karl, D.M. (2008) Nitrogen fixation rates and
342 controls at Stn ALOHA. *Aq Microb Ecol* **52**:175–183.
343 Graham B.M., Hamilton, R.D., and Campbell, N.E.R (1980) Comparison of the nitrogen-
344 15 uptake and acetylene reduction methods for estimating the rates of nitrogen fixation
345 by freshwater blue-green algae. *Can. J. Microbiol*. **37**:488–493.
346 Herr, F.L., Frank, E.C., Leones, G.M., and Kennicutt, M.C. (1984) Diurnal variability of
347 dissolved molecular hydrogen in the tropical South Atlantic Ocean. *Deep-Sea Res* **31**:
348 13–20.
349 Jähne, B., Heinz, G., and Dietrich, W. (1987) Measurement of the diffusion coefficients
350 of sparingly soluble gases in water. *J Geophys Res **92***: 10,767–10,775.
351 Ledwell, J.R., A.J. Watson and C.S. Law (1993) Evidence for slow mixing across the
352 pycnocline from an open-ocean tracer-release experiment. *Nature* **364**: 701–703.
353 Levitus, S. (1982) Climatological atlas of the world ocean. National Oceanic and
354 Atmospheric Administration. Professional Paper 13, Rockville, MD., pp 1–173.
355 Mague, T.H., Mague, F.C., and Holm-Hansen, O. (1977) Physiology and chemical
356 composition of nitrogen-fixing phytoplankton in the central North Pacific Ocean. *Mar*
357 *Biol* **41**: 213–227.

Moisander, P.H., Beinart, R.A., Hewson, I., White, A.E., Johnson, K.S., Carlson, C.A., Montoya, J.P., and Zehr, J.P. (2010) Unicellular cyanobacterial distributions broaden the oceanic N_2 fixation domain. *Science* **327**:1512–14.

Montoya, J.P., Voss, M., Kähler, P., and Capone, D.G. (1996) A simple, high-precision, high-sensitivity tracer assay for N_2 fixation. *Appl Environ Microbiol* **62**: 986–993.

Moore, R.M., Punshon, S., Mahaffey, C., and Karl, D.M. (2009) The relationship between dissolved hydrogen and nitrogen fixation in ocean waters. *Deep-Sea Res* **56:** 1449–1458.

Mulholland, M.R., Bronk, D.A, and Capone, D.G. (2004) Dinitrogen fixation and release of ammonium and dissolved organic nitrogen by *Trichodesmium* IMS101. *Aq Microb Ecol* **37**: 85–94.

Novelli, P.C., Lang, P.M., Masarie, K.A., Hurst, D.F., Myers, R., and Elkins, J.W. (1999) Molecular hydrogen in the troposphere: Global distribution and budget. *J. Geophys. Res.* **104**: 30,427–30,444.

Paerl, H.W. (1982) *In situ* H_2 production and utilization by natural populations of N_2-fixing blue-green algae. *Canadian J Botany* **60**: 2542–2546.

Paerl, H.W. (1983) Environmental regulation of H_2 utilization ($^3H_2$ exchange) among natural and laboratory populations of N_2 and non-N_2 fixing phytoplankton. *Microb Ecol* **9**: 79–97.

Price, H., Jaeglé, L., Rice, A., Quay, P., Novelli, P.C., and Gammon, R. (2007) Global budget of molecular hydrogen and its deuterium content:constraints from ground station, cruise, and aircraft observations. *J Geophys Res* **112**: D22108, doi:10.1029/2006JD008152.

Punshon, S., Moore, R.M., and Xie, H. (2007) Net loss rates and distribution of molecular hydrogen (H_2) in mid-latitude coastal waters. *Mar Chem* **105**: 129–139.

Punshon, S., and Moore, R.M. (2008) Photochemical production of molecular hydrogen in lake water and coastal seawater, *Mar Chem* **108**: 215–220.

Schropp, S.J., Scranton, M.I., and Schwarz, J.R. (1987) Dissolved hydrogen, facultatively anaerobic, hydrogen-producing bacteria, and potential hydrogen production rates in the western North Atlantic Ocean and Gulf of Mexico. *Limnol Oceanogr* **32**: 396–402.

Schubert, K.R., and Evans, H.J. (1976) Hydrogen evolution: A major factor affecting the efficiency of nitrogen fixation in nodulated symbionts. *Proc Nat Acad Sci USA* **73**: 1207–1211.

Scranton, M.I., Jones, M.M., and Herr, F.L. (1982) Distribution and variability of dissolved hydrogen in the Mediterranean Sea. *J Mar Res* **40**: 873–891.

Scranton, M.I., Novelli, P.C., Michaels, A., Horrigan, S.G., and Carpenter, E.J. (1987) Hydrogen production and nitrogen fixation by *Oscillatoria thiebautii* during in situ incubations. *Limnol Oceanogr* **32**: 998–1006.

Simpson, F.B., and Burris, R.H. (1984) A nitrogen pressure of 50 atmospheres does not prevent evolution of hydrogen by nitrogenase. *Science* **224**: 1095–1097.

Tamagnini, P., Leitão, E., Oliveira, P., Ferreira, D., Pinto, F., Harris, D.J., Heidorn, T., and Lindblad, P. (2007) Cyanobacterial hydrogenases: diversity, regulation and applications. *FEMS Microbiol Reviews* **31**: 692–720.

Wanninkhof, R. (1992) Relationship between gas exchange and wind speed over the ocean. *J Geophys Res* **97**: 7373–7381.

403 Waterbury, J.B., Watson, S.W., and Valois, F.W. (1988) Temporal separation of
404 photosynthesis and dinitrogen fixation in the marine unicellular cyanobacterium:
405 *Erythrosphaera marina*. *EOS Transactions, American Geophys Union* **69**: 1089.
406 Wiesenburg, D.A., and Guinasso, N.L. (1979) Equilibrium solubilities of methane,
407 carbon monoxide and hydrogen in water and seawater. *J Chem Eng Data* **24**: 356–360.
408 Wilson, S.T., Foster, R.A., Zehr, J.P., and Karl, D.M. (2010) Hydrogen production by
409 *Trichodesmium erythraeum, Cyanothece* sp. and *Crocosphaera watsonii*. *Aq Microb Ecol*
410 **59**: 197–206.
411 Wilson, S. T., Böttjer, D., Church, M. J., and Karl, D. M. (2012a) Comparative
412 assessment of nitrogen fixation methodologies conducted in the oligotrophic North
413 Pacific Ocean. *Appl Environ Microbiol* **78**: 6516–6523.
414 Wilson, S.T., Kolber, Z.S., Tozzi, S., Zehr, J.P., and Karl, D.M. (2012b) Nitrogen
415 fixation, hydrogen production and electron transport kinetics in *Trichodesmium*
416 *erythraeum* strain IMS101. *J Phycol* **48**:595–506.
417 Zehr, J.P., Waterbury, J.B., Turner, P.J., Montoya, J.P., Omoregie, E., Steward, G.F.,
418 Hansen, A., and Karl, D.M. (2001) Unicellular cyanobacteria fix N_2 in the subtropical
419 North Pacific Ocean. *Nature* **412**: 635–638.

Tables

Table 1. Rates of biological $^3H_2$ oxidation conducted on whole seawater samples collected at 25 m (the error bars represent standard deviation of replicate samples, n=3). The rate measurements are compared with the $^{15}N_2$ assimilation and C_2H_4 production values in whole seawater (Fig. 1) to calculate the percentage of N_2 fixation accounted for by biological oxidation.

Station sampled	Water-column $^3H_2$ oxidation (pmol H_2 L^{-1} h^{-1})	% of AR assay accounted for by $^3H_2$ oxidation	% of $^{15}N_2$ assimilation accounted for by $^3H_2$ oxidation	Turnover time of dissolved H_2 pool (h)
Stn 3 (Day)	15 ± 1	0.8	18.8	40
Stn 3 (Night)	25 ± 4	0.9	11.4	23
Stn 13 (Day)	42 ± 6	1.3	16.2	22
Stn 13 (Night)	25 ± 2	6.6	62.5	36

Table 2. Estimation of H_2 production in the open ocean water-column at a depth of 25 m. The minimum and maximum values are based on 1 and 25 % of C_2H_4 production.

Date sampled	Water-column H_2 concentration (nmol H_2 L^{-1})	AR assay (nmol C_2H_4 L^{-1} h^{-1})	Estimated H_2 prod. (nmol H_2 L^{-1} h^{-1}) Min.	Max.	Estimated time to replenish H_2 stock (h)
Stn 3 (Day)	0.6	1.77	0.018	0.44	1 – 34
Stn 3 (Night)	0.6	2.87	0.029	0.72	1 – 21
Stn 13 (Day)	0.93	3.34	0.033	0.84	1 – 28
Stn 13 (Night)	0.93	0.38	0.004	0.10	10 – 245

Table 3. Estimates of sea-air gas flux, downwards diffusion, and biological consumption in comparison with depth-integrated (0-45 m) dissolved H_2 concentrations.

Date	Depth-integrated (0-45 m) H_2 concentrations (µmol m^{-2})	Water-column Sea-air H_2 flux (µmol H_2 m^{-2} h^{-1})	Downward diffusion (µmol H_2 m^{-2} h^{-1})	Biological consumption (µmol H_2 m^{-2} h^{-1})
Stn 3 (Day)	30.6	0.03 - 0.06	0.42	0.03 - 5.17
Stn 3 (Night)	30.6	0.04 - 0.08	0.42	0.31 - 3.87
Stn 13 (Day)	41.0	0.11 - 0.37	0.68	0.47 - 5.80
Stn 13 (Night)	41.0	0.08 - 0.33	0.68	1.69 - 16.05

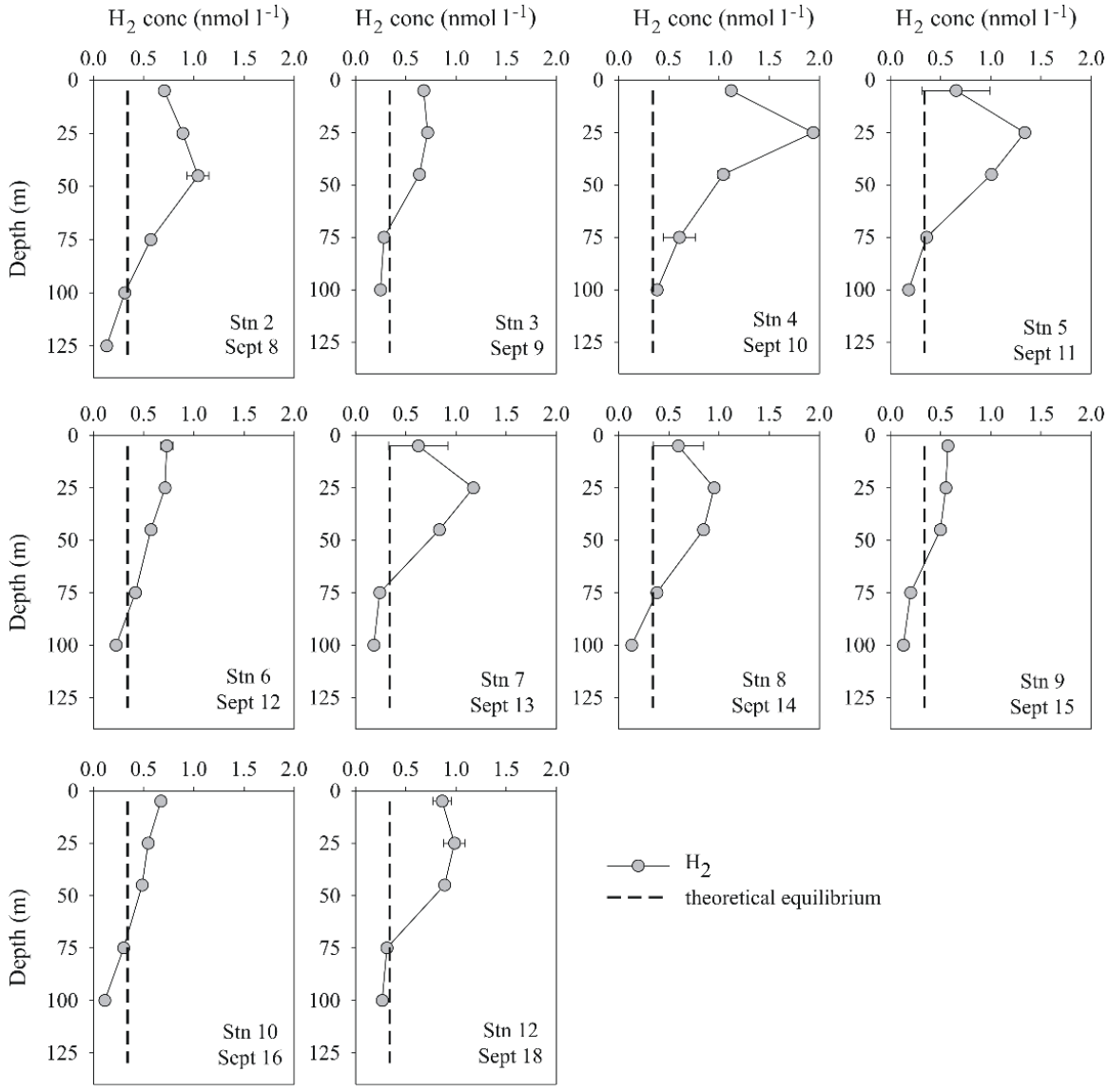

460

461 Figure 1. Dissolved H_2 concentrations (nmol l^{-1}) between depths of 5 to 125 m in the
462 North Pacific Ocean. For each sampling occasion, seawater samples were collected at
463 1300 hrs. The theoretical value of dissolved H_2 concentrations in seawater at
464 atmospheric equilibrium (with an atmospheric concentration of 0.5 ppmv) is represented
465 by the dashed line. Error bars where shown represent standard deviation (n=3).

466

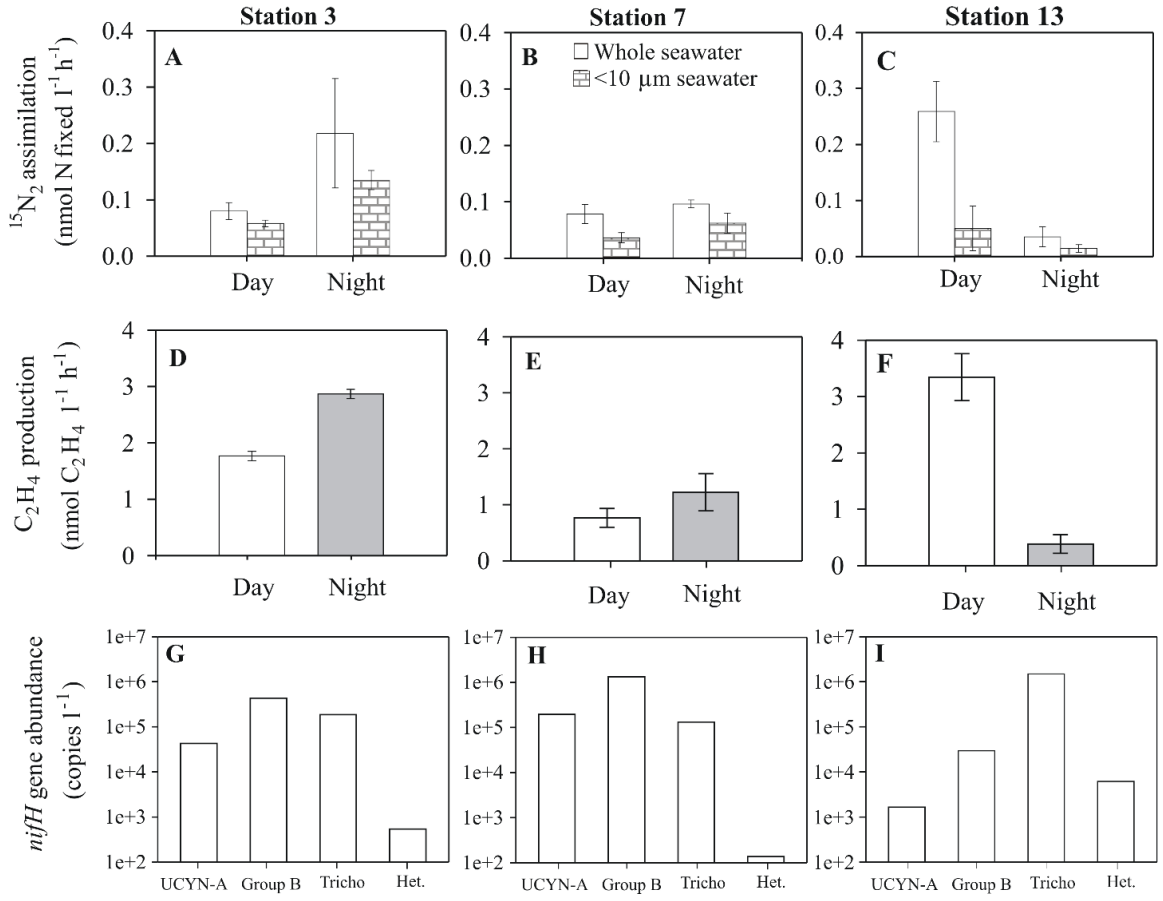

Figure 2. N_2 fixation rates as measured by (A-C) $^{15}N_2$ tracer assimilation and (D-F) the AR assay for seawater samples collected at 25 m and incubated onboard the ship during either the day or night period. Post-incubation size-fractionation was conducted for replicate $^{15}N_2$ tracer additions and not for the AR assay. The error bars in A-F represent standard error (n=3). The *nifH* gene abundances collected from the same depth on the same date are shown for UCYN-A, Group B (*Crocosphaera* spp.), (Tricho) *Trichodesmium* and (het) heterocystous cyanobacteria (G-I).

Supplementary Information

Water column structure and biogeochemical properties

Shipboard sampling was conducted in the North Pacific Subtropical Gyre along a cruise track which transited the edge of two anticyclonic mesoscale eddies (Fig S1). A total of 11 sampling stations were occupied during the cruise, spanning a total distance of approximately 170 km. To characterize the upper water column, vertical profiles were conducted using a Conductivity-Temperature-Depth (CTD) system coupled to a rosette consisting of 24 x 12 liter Niskin-like 'Bullister' bottles. Oxygen (O_2) and fluorescence sensors were calibrated against discrete measurements of dissolved O_2 (Carritt and Carpenter, 1966) and chlorophyll *a* (chl *a*) extracted and analyzed by fluorometry (Turner AU-10). Seawater for determination of nutrient concentrations (NO_2^- + NO_3^-, SRP, and Si) was subsampled into acid washed 125 ml polyethylene bottles, capped, and then stored frozen. Sample analysis was performed on land as documented in the online manual for "HOT Laboratory Protocols" (*http://hahana.soest.hawaii.edu*).

An overview of the water-column biogeochemistry is provided by comparing vertical profiles of nutrients and chl *a* from Stn 3 (24° 43.4′ N, 157° 33.2′ W) during the first part of the transect and from Stn 13 (24° 48′ N, 158° 15.2′ W) during the latter part of the transect (Fig. S1). At Stn 3, the maximum chl *a* concentrations were observed at a depth of 115 m, compared to a depth of 105 m at Stn 13 (Fig. 2). The nutrient profiles revealed a significant difference between concentrations of silicate (Si) (one-tailed t-test, P=0.04) and soluble reactive phosphorus (SRP) (one-tailed t-test, P=0.03) in the surface mixed layer (0–45m) between Stn 3 and 13. Furthermore, the vertical profile of SRP concentrations at Stn 3 revealed a distinct subsurface minimum with concentrations

decreasing from 0.09 µM at 25 m to 0.02 µM at 100 m. Beneath 100 m, the concentrations of nitrate + nitrite (NO_3^- + NO_2^-), Si, and SRP increased more rapidly with depth at Stn 13 where concentrations were 16, 42, and 210% higher than Stn 3 by 175 m, respectively (Fig. S2).

H_2 measurements

Discrete seawater samples for measuring dissolved H_2 concentrations were collected into acid-washed, glass-stoppered 300 ml Wheaton bottles. Samples were analyzed immediately after collection with a total sample processing time of <2 h. To quantify H_2 concentrations, seawater was sub-sampled from the Wheaton bottles into a 50 ml glass syringe (Perfektum) via 1/8″ polyetheretherketone (PEEK) tubing. The syringe was flushed twice with sample water, ensuring the last flush was free of air bubbles. A custom-built syringe actuator ensured that a consistent volume of seawater (35 ml) was always introduced into the syringe. Subsequently 5 ml of H_2-free (<10 parts per trillion) air (Airgas) was introduced into the syringe, H_2 was extracted from the seawater using headspace equilibration, and the headspace was subsequently injected into the gas analyzer (described below). To prevent accidental addition of seawater following after the headspace injection, the sampling inlet for the analyzer was fitted with a hydrophobic syringe filter (13 mm PTFE membrane, 0.2 µm pore size).

We note that the samples are not preserved and therefore H_2 concentrations could potentially change between the time of collection and analysis. The likelihood of this occurring in oligotrophic seawater samples within < 2 h of sample collection is considered minimal. The analysis of replicate samples in random order on previous

523 occasions did not result in any significant increase in the standard deviation of replicate
524 (typically 3) seawater samples. Also whilst this study shows that production of H_2 via N_2
525 fixation can replenish the dissolved H_2 pool in 1-38 h, we consider the upper estimate of
526 1 h to be high and the median value of 18 h to be more reasonable which exceeds the 1-2
527 h required for processing all samples.
528 H_2 was quantified with a reduced gas analyzer that couples a mercuric oxide (HgO)
529 bed to a reducing compound photometer (Peak Laboratories, USA). The stoichiometric
530 reduction of HgO by H_2 gas releases mercury vapor which is quantified using an
531 ultraviolet absorption photometer located immediately downstream of the HgO bed. For
532 safety purposes, the gas flow exiting the detector passes through an activated charcoal
533 mercury vapor scrubber before venting to the atmosphere. Prior to the detector, the
534 carrier gas (Ultra High Purity air) passes through two analytical columns maintained at
535 104 ^{o}C. The first column is packed with Unibeads 1S (60/80 mesh, 0.32 cm diameter and
536 41.9 cm length), and the second column with Molecular Sieve 13X (60/80 mesh, 0.32 cm
537 diameter and 206 cm length). The analytical precision based on the comparison of 4
538 samples at atmospheric equilibrium (0.3 nmol l^{-1}) was ± 2%. The analyzer was calibrated
539 using a 1 ppmv H_2 standard (Scott Marrin) that was diluted up to 100-fold using zero-H_2
540 air. The concentration of dissolved H_2 in equilibrated seawater was calculated according
541 to the Bunsen solubility coefficients provided by Wiesenburg and Guinasso (1979).
542 On two separate occasions, the rate of H_2 consumption was quantified by measuring
543 the production of $^{3}H_2O$ from tracer additions (0.024–0.046 nM) of $^{3}H_2$. This method has
544 previously been used to measure $^{3}H_2$ uptake in laboratory cultures of diazotrophs (Chan
545 *et al*., 1980) and environmental microbial assemblages (Paerl, 1983). The seawater

546 sample was collected in a 40 ml borosilicate glass vial with 2–3 times overflow and
547 sealed with no headspace using Teflon-faced butyl rubber stoppers. Tritium gas (specific
548 activity: 2 TBq/mmol; ViTrax, California) was injected into the vial in tracer quantities
549 (10 to 25 pM) and shaken before quickly venting non-dissolved $^3H_2$ in a fume hood.
550 Seawater samples amended with $^3H_2$ were incubated for 4 h in the deckboard incubators
551 at repeated intervals during the day and night periods of a diel cycle. Samples were
552 analyzed in triplicate with control samples for abiotic conversion of $^3H_2$ consisting of 0.2
553 µm filtered seawater. No activity was observed in the control samples during the
554 experiments. At the end of the incubation, a 1 ml sub-sample was removed using a
555 syringe and injected into a scintillation vial containing scintillation cocktail (Ultima Gold
556 LLT, Perkin Elmer) and counted immediately in a liquid scintillation analyzer (Tri-Carb
557 2910 TR, Perkin Elmer) to determine the total activity added to the sample. To quantify
558 the amount of transformed $^3H_2$, a separate 2 ml subsample was added to a scintillation
559 vial and purged with N_2 (100 ml min^{-1} for 3 min) in a fume hood to remove any
560 remaining $^3H_2$. A 1 ml aliquot of the sparged samples was subsequently pipetted into a
561 second scintillation vial containing liquid scintillation cocktail and counted. To account
562 for isotopic discrimination effects when calculating the rate of H_2 oxidation, we used the
563 fractionation factor reported in Soffiento *et al*. (2006). It should be noted that as
564 acknowledged by Soffiento *et al*. (2006), fractionation effects may vary between the
565 different hydrogenase enzymes *e.g*. iron(Fe)-only hydrogenase compared to the nickel-
566 iron (NiFe) hydrogenases contained by cyanobacteria (Tamagnini *et al*., 2007). This
567 should be resolved by analyzing the fractionation factor in phylogenetically distinct

hydrogenase-containing microorganisms before assessing the consequences of measuring $^{3}H_2$ oxidation in mixed microbial assemblages.

N_2 fixation rate measurements

Rates of N_2 fixation were measured using both the $^{15}N_2$ tracer technique and the acetylene reduction (AR) assay at three sampling stations: Stn 3, 7, and 13, which were occupied on the 9, 13, and 19 September, respectively. The AR assay was conducted using a reduced gas analyzer, similar to the instrument described in '*H_2 measurements*', for the quantification of C_2H_4 production (Wilson *et al*., 2012). The increased sensitivity (5 pmol l^{-1}) provided by the reducing compound photometer compared to standard C_2H_4 quantification using gas chromatography-flame ionization detector (GC-FID) permits the AR assay to be conducted on seawater samples with no preconcentration of the biomass. Control treatments consisted of 0.2 µm filtered surface seawater, analyzed in triplicate alongside the regular seawater samples. The blank to signal ratio, indicative of the biological production relative to the background presence of C_2H_4 ranged from 75–82%. Both samples and controls were incubated using deckboard incubators with typical incubation periods of 3–4 h.

Alongside the AR assay the rate of $^{15}N_2$ assimilation into particulate biomass was also measured in seawater samples. The $^{15}N_2$ tracer was added to seawater samples as '$^{15}N_2$ enriched seawater', prepared onboard the ship by filtering seawater collected from 25 m through a 0.2 µm filter, followed by vacuum degasification (250 mbar for 40 min). The $^{15}N_2$ gas (98% purity; Isotech Laboratories, Inc.) was dissolved in the sterile, degassed seawater and 50 ml of $^{15}N_2$ enriched seawater was added to the seawater samples in 4.3

liter polycarbonate bottles to give a final $^{15}N_2$ enrichment of 1.5 atom%. Samples were incubated in the presence of $^{15}N_2$ tracer for either 11 h or 13 h corresponding to the day/night-time, respectively. Seawater samples designated for night-time analysis were collected at the same time as the day-time samples and incubated without tracer additions until spiked with $^{15}N_2$ enriched seawater at 2000 hrs. Post-incubation, the seawater samples were filtered onto combusted 25 mm glass fiber filters as both unfiltered (whole) seawater and the <10 µm size fraction (representing UCYN-A and Group B). The samples were then stored at -20^{o}C prior to analysis on land to quantify the $^{15}N_2$ enrichment of particulate material using an elemental analyzer-isotope ratio mass spectrometer, as described in Montoya *et al*. (1996).

Molecular analysis of nifH

Discrete seawater samples (2–4 liters) were collected at 1300 hrs using the CTD-rosette from a depth of 25 m, filtered using a peristaltic pump through a 0.22 µm Sterivex filter (Millipore, Billerica, MA, USA) and stored in liquid N_2. A full description of methodological protocols including DNA extraction and quantitative PCR analyses has been previously published by Moisander *et al*. (2010).

610 References

611 Carritt, D.E., and Carpenter, J.H. (1966) Comparison and evaluation of currently
612 employed modifications of the Winkler method for determining dissolved oxygen is
613 seawater: a NASCO report. *J Mar Res* **24**: 286–318.

614 Chan, Y.K., Nelson, L.M., and Knowles, R. (1980) Hydrogen metabolism of
615 *Axospirillum brasilense* in nitrogen-free medium. *Can J Microbiol* **26**: 1126–1131.

616 Levitus, S. (1982) Climatological atlas of the world ocean. National Oceanic and
617 Atmospheric Administration. Professional Paper 13, Rockville, MD., pp 1–173.

618 Montoya, J.P., Voss, M., Kähler, P., and Capone, D.G. (1996) A simple, high-precision,
619 high-sensitivity tracer assay for N_2 fixation. *Appl Environ Microbiol* **62**: 986–993.

620 Paerl, H.W. (1983) Environmental regulation of H_2 utilization ($^3H_2$ exchange) among
621 natural and laboratory populations of N_2 and non-N_2 fixing phytoplankton. *Microb Ecol*
622 **9**: 79–97.

623 Scholin, C. (2010) What are 'ecogenomic sensors?' A review and thoughts for the future.
624 *Ocean Sci* **6**: 51–60.

625 Soffientino, B., Spivack, A.J., Smith, D.C., Roggenstein, E.B., and D'Hondt, S. (2006) A
626 versatile and sensitive tritium-based radioassay for measuring hydrogenase activity in
627 aquatic sediments. *J Microbiol Methods* **66**: 136–146.

628 Wiesenburg, D.A., and Guinasso, N.L. (1979) Equilibrium solubilities of methane,
629 carbon monoxide and hydrogen in water and seawater. *J Chem Eng Data* **24**: 356–360.

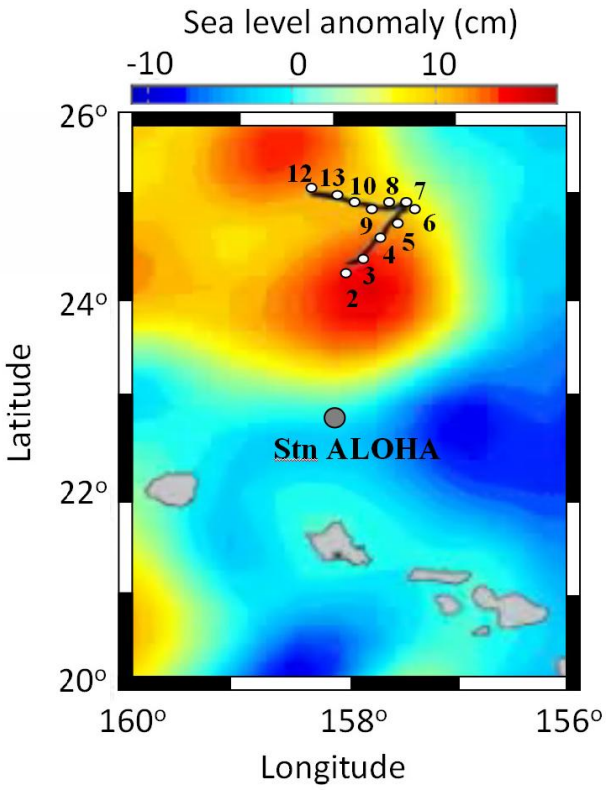

630

631 Figure S1. 14 day composite of satellite derived SSHA 100 km north of the Hawaiian

632 Islands in the Pacific Ocean between 7-21 September 2011 (data from Moderate

633 Resolution Imaging Spectroradiometer). A summary of the cruise transect is indicated by

634 the solid black line and the labeled white circles represent the sampling stations discussed

635 in the text. Station ALOHA, the long term sampling station for the Hawaii Ocean Time-

636 series (HOT) program, located at 22 ^{o} 45' N, 158^{o} W is also highlighted.

637

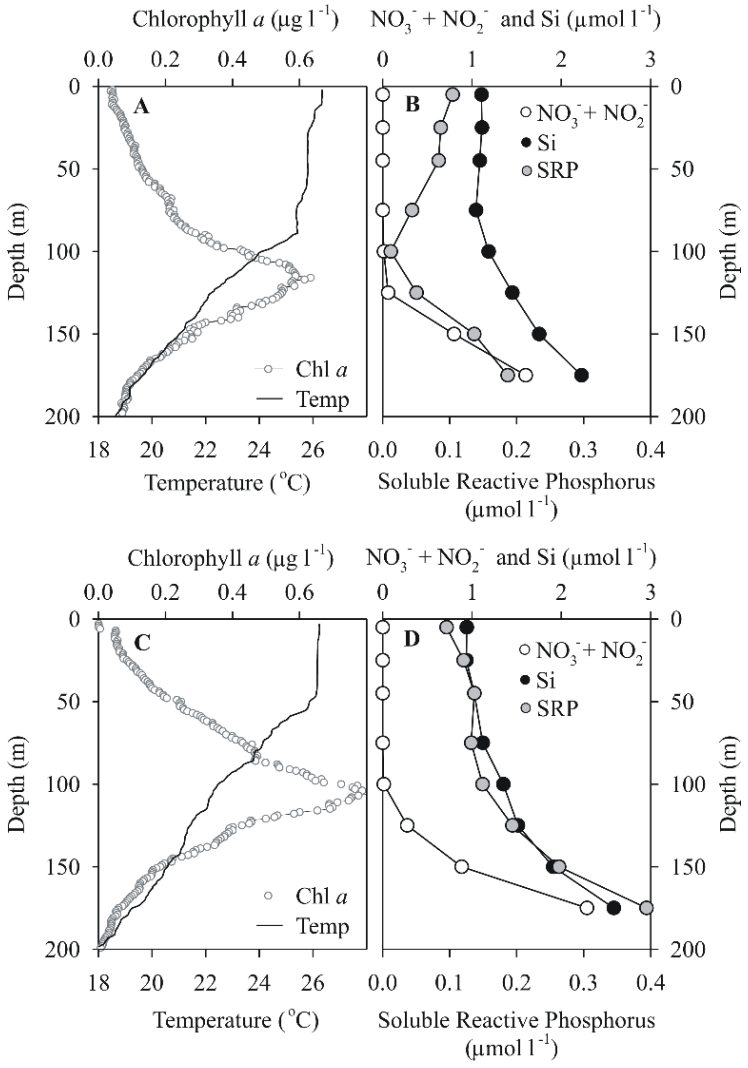

638

639 Figure S2. Representative water column profiles for the two sections of the cruise track,

640 (A-B) Stn 3 and (C-D) Stn 13.